THE RADIO SPECTRAL INDEX AND EXPANSION OF 3C 58

M. F. BIETENHOLZ,

Department of Physics and Astronomy, York University, Toronto M3J 1P3, Ontario, Canada; michael@polaris.phys.yorku.ca

AND

N. E. KASSIM AND K. W. WEILER

Code 7213, Naval Research Laboratory, Washington, DC 20375-5320

Received 2001 April 27; accepted 2001 June 25

ABSTRACT

We present new observations of the plerionic supernova remnant 3C 58 with the VLA at 74 and 327 MHz. In addition, we re-reduced earlier observations at 1.4 and 4.9 GHz taken in 1973 and 1984. Comparing these various images, we find that (1) the remnant has a flat and relatively uniform spectral-index distribution, (2) any expansion of the remnant with time is significantly less than that expected for uniform, undecelerated expansion since the generally accepted explosion date in 1181 A.D., and (3) there is no evidence for a nonthermal synchrotron-emission shell generated by a supernova shock wave, with any such emission having a surface brightness of less than 1×10^{-21} W m^{-2} Hz^{-1} sr^{-1} at 327 MHz.

Subject headings: ISM: individual (3C 58) — radio continuum: ISM — supernova remnants

1. INTRODUCTION

Plerionic, or filled-center, supernova remnants (Weiler & Panagia 1978; Weiler & Sramek 1988) have become established as a class. The supernova remnant 3C 58 (G130.7+3.1) was an early member of the class, and it has often been described as morphologically similar to the Crab Nebula, the Crab being the prototype for this class. 3C 58 is at a similar distance as the Crab, 3.2 kpc (Roberts et al. 1993), has a similar size, $6' \times 9'$, and shows a similar filamentary, filled-center morphology in the radio (Weiler & Seielstad 1971; Wilson & Weiler 1976; Green 1986; Reynolds & Aller 1988). Like the Crab, 3C 58 has a relatively flat radio spectrum, with $\alpha = -0.10 \pm 0.02$ ($S \propto \nu^{+\alpha}$), from 40 MHz to 15 GHz (Wilson & Weiler 1976; Green 1986). 3C 58 has been moderately well identified with the historical supernova event of 1181 A.D. (Clark & Stephenson 1977), which would give it an age similar to that of the Crab, which is associated with SN 1054.

Plerions are thought to be powered by pulsars, which build their nonthermal nebulae through the injection of relativistic particles and the amplification of magnetic fields, although the exact injection and acceleration processes are not yet well understood. In the optical, radial velocities less than 900 km s^{-1} have been measured for the filaments in 3C 58 (Fesen 1983), which is consistent with the association with SN 1181 only if the remnant has been substantially decelerated or if the filaments are due to the excitation of in situ matter overrun by the supernova shock. However, the linear size of less than 9 pc (for a distance of 3.2 kpc), along with the age of only 820 yr, implies rather low expansion velocities, which suggests a low-energy supernova event. In addition, the radio flux density has been shown to be *increasing* (Aller & Reynolds 1985; Aller, Aller, & Reynolds 1986; Green 1987). It seems (Salvati et al. 1998; Woltjer et al. 1997) that a nonstandard evolution of the pulsar's output is required to reconcile this and the relatively low frequency of the observed spectral break in the synchrotron emission (Green & Scheuer 1992) with an age of 820 yr.

2. OBSERVATIONS AND DATA REDUCTION

We observed 3C 58 using the A and B configurations of NRAO's Very Large Array (VLA) at 74 MHz using 63 spectral channels for a total bandwidth of 1.5 MHz, and at 327 MHz using 31 spectral channels for a total bandwidth of 3 MHz. Spectral-line mode was used to be able to excise radio frequency interference (RFI).

The data were calibrated and reduced using NRAO's AIPS software package. The instrumental bandpass was determined using observations of Cyg A. The amplitude gains were set using Cyg A at 74 and 3C 48 at 327 MHz, and were tied to the flux scale of Baars et al. (1977). Reduction of 74 MHz data requires somewhat different techniques.[1] In particular, RFI is a significant problem, and the data were first automatically edited for deviant samples in frequency space by the AIPS task SPFLG. We then averaged the data into a manageable number of channels and further edited each channel manually.

Sidelobes from sources well outside the primary beam are a significant problem at 74 MHz, and Cas A, which was 20° away, produced strong sidelobes in our field of view. In order to correctly remove these sidelobes, three-dimensional imaging was required (see Perley 1999), and the AIPS task IMAGR was used to simultaneously image and deconvolve numerous flat but noncoplanar regions. These were then reassembled into a single image by the task FLATN.

3. RESULTS

3.1. *Images*

The full-resolution image at 74 MHz is shown in Figure 1. This image is made from the combined A- and B-array data sets with uniform weighting, and has a restoring beam size of 26″ (FWHM). The peak brightness for 3C 58 is 0.55 Jy beam^{-1}, the background rms is 20 mJy beam^{-1}, and the total flux density for 3C 58 is 33.6 Jy. The image at 327 MHz is shown in Figure 2. It is made from the combined A- and B-array data sets, and has a restoring beam size of 8″.2 (FWHM), a peak brightness for 3C 58 of 63 mJy beam^{-1}, a background rms of 0.57 mJy beam^{-1}, and a total flux density for 3C 58 of 33.9 Jy. It should be noted that no compact emission source is detected near the center of the nebula. In addition, in Figure 3, we show a low-resolution

---

[1] For a tutorial, see http://rsd-www.nrl.navy.mil/7213/lazio/tutorial.

		Form Approved OMB No. 0704-0188

Report Documentation Page

Form Approved
OMB No. 0704-0188

Public reporting burden for the collection of information is estimated to average 1 hour per response, including the time for reviewing instructions, searching existing data sources, gathering and maintaining the data needed, and completing and reviewing the collection of information. Send comments regarding this burden estimate or any other aspect of this collection of information, including suggestions for reducing this burden, to Washington Headquarters Services, Directorate for Information Operations and Reports, 1215 Jefferson Davis Highway, Suite 1204, Arlington VA 22202-4302. Respondents should be aware that notwithstanding any other provision of law, no person shall be subject to a penalty for failing to comply with a collection of information if it does not display a currently valid OMB control number.

1. REPORT DATE **OCT 2001**	2. REPORT TYPE	3. DATES COVERED **00-00-2001 to 00-00-2001**
4. TITLE AND SUBTITLE **The Radio Spectral Index and Expansion of 3C 58**		5a. CONTRACT NUMBER
		5b. GRANT NUMBER
		5c. PROGRAM ELEMENT NUMBER
6. AUTHOR(S)		5d. PROJECT NUMBER
		5e. TASK NUMBER
		5f. WORK UNIT NUMBER
7. PERFORMING ORGANIZATION NAME(S) AND ADDRESS(ES) **Naval Research Laboratory,Code 7213,4555 Overlook Avenue, SW,Washington,DC,20375**		8. PERFORMING ORGANIZATION REPORT NUMBER
9. SPONSORING/MONITORING AGENCY NAME(S) AND ADDRESS(ES)		10. SPONSOR/MONITOR'S ACRONYM(S)
		11. SPONSOR/MONITOR'S REPORT NUMBER(S)
12. DISTRIBUTION/AVAILABILITY STATEMENT **Approved for public release; distribution unlimited**		
13. SUPPLEMENTARY NOTES		
14. ABSTRACT		
15. SUBJECT TERMS		

16. SECURITY CLASSIFICATION OF:			17. LIMITATION OF ABSTRACT	18. NUMBER OF PAGES **7**	19a. NAME OF RESPONSIBLE PERSON
a. REPORT **unclassified**	b. ABSTRACT **unclassified**	c. THIS PAGE **unclassified**			

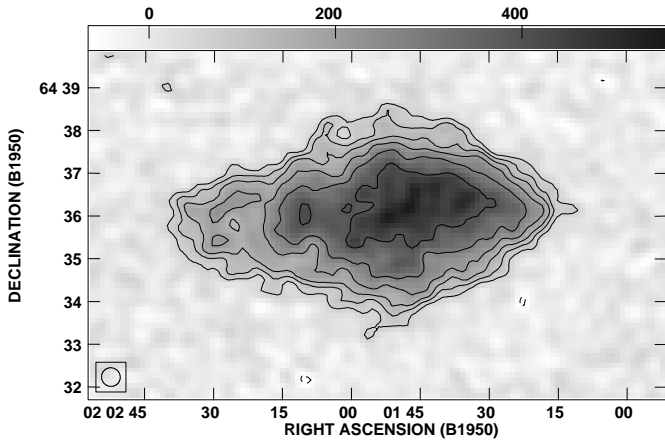**Standard Form 298 (Rev. 8-98)**
Prescribed by ANSI Std Z39-18

Fig. 1.—Image of 3C 58 at 74 MHz from combined VLA A- and B-array data. The FWHM resolution is 26″ and is indicated at lower left, the peak brightness is 0.55 Jy beam^{-1}, and the background rms is 20 mJy beam^{-1}. The gray scale is in mJy beam^{-1}. The contours are drawn at −6%, 6%, 10%, 14.1%, 20%, 28.2%, and 40% of the peak brightness.

Fig. 3.—Low-resolution image of the region surrounding 3C 58 at 327 MHz. The image has been convolved with a Gaussian of 3′.3 FWHM, corrected for the primary beam response, and blanked where the primary beam response is less than 50%. The peak flux in the image is 15.9 Jy beam^{-1}. The background rms ranges from ∼20 mJy beam^{-1} near 3C 58 to ∼45 mJy beam^{-1} near the edge of the field of view. The gray scale is in mJy beam^{-1}.

image of the whole primary beam area at 327 MHz, convolved to a resolution of 3′.3. No shell emission is visible. The average background rms between the edge of the field and the center is 37 mJy beam^{-1}, or 3.4×10^{-22} W m^{-2} Hz^{-1} sr^{-1}. We can accordingly place a 3σ limit on any shell emission of 1×10^{-21} W m^{-2} Hz^{-1} sr^{-1} at 327 MHz. While the field of view at 74 MHz is even larger, the sensitivity is considerably poorer, so the higher frequency gives our most sensitive limit on extended emission. We note however, that the 74 MHz observations would be sensitive to very large shells, i.e., with diameters greater than 1°.5, and we see no such shell emission.

3.2. *Spectral Index Distribution*

We made an image of the spectral index between 74 and 327 MHz,[2] $\alpha_{0.07}^{0.33}$, as follows. The 327 MHz image was convolved to the larger resolution at 74 MHz, and then the two

---

[2] We refer to spectral indices with sub- and superscripts indicating the relevant frequencies in GHz.

images were aligned by the peaks of the point sources near 3C 58 (at 74 MHz, ionospheric refraction can cause substantial displacement of the entire image). This image of $\alpha_{0.07}^{0.33}$, which has a resolution of 26″, is shown in Figure 4 (regions where the uncertainty in $\alpha_{0.07}^{0.33}$ is larger than 0.4 have been blanked for clarity). The spectral index has a mean value of −0.04 over the nebula, with an rms of 0.18. Only random variations are visible in Figure 4. In particular, no steepening toward the edge of the nebula is observed.

We can calculate the integrated value of $\alpha_{0.07}^{0.33}$ from the total flux densities in the naturally weighted images, and we obtain $\alpha_{0.07}^{0.33}$ (integrated) = -0.07 ± 0.05, where the uncertainty comes chiefly from the uncertainty in the VLA ampli-
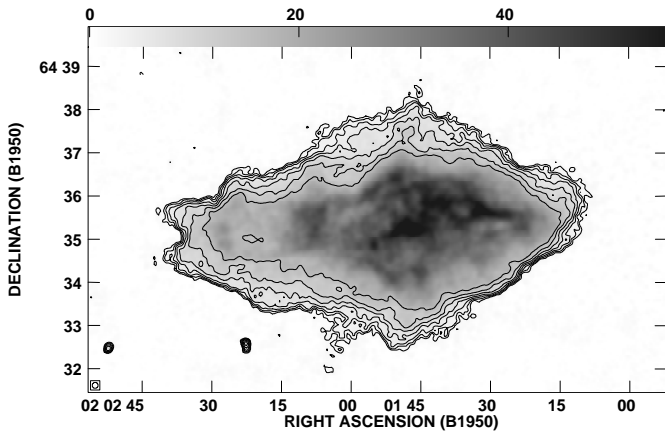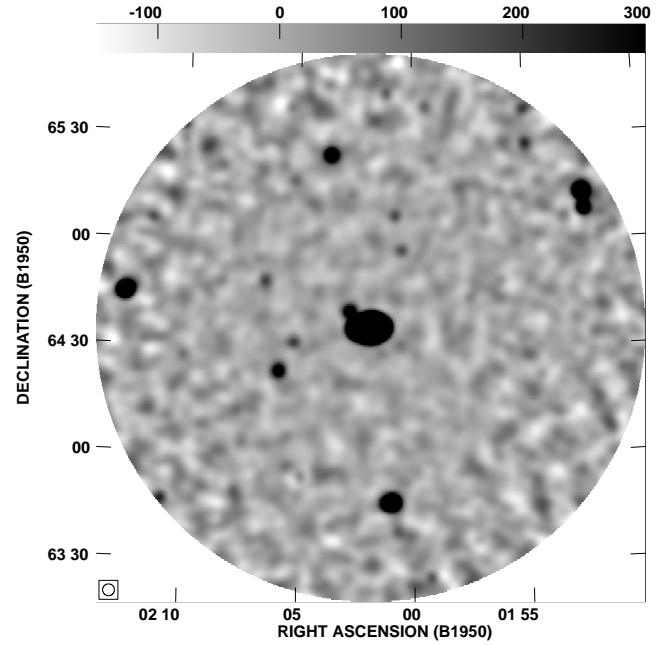

Fig. 2.—Image of 3C 58 at 327 MHz from VLA A- and B-array data. The FWHM resolution is 8″.2 and is indicated at lower left, the peak brightness is 63 mJy beam^{-1}, and the background rms is 0.57 mJy beam^{-1}. The gray scale is in mJy beam^{-1}. The contours are drawn at −2, 2, 2.8, 4, 5.7, 8, 11.3, and 16 mJy beam^{-1}.
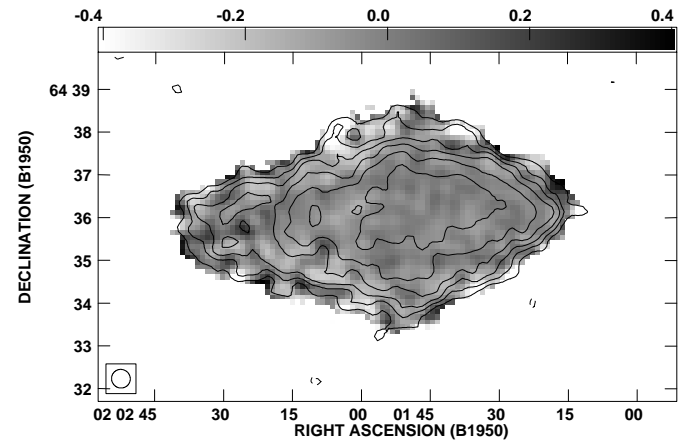

Fig. 4.—Radio spectral index of 3C 58 between 74 and 327 MHz, $\alpha_{0.07}^{0.33}$, shown in gray scale. The FWHM resolution is 21″ (shown at lower left). For reference, we repeat the total intensity contours from Fig. 1.
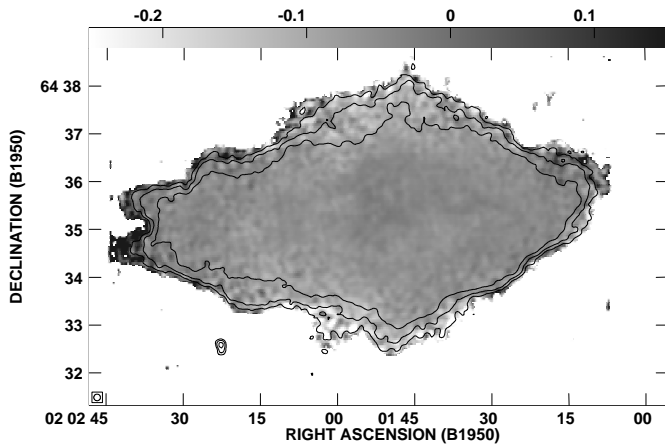
FIG. 5.—Radio spectral index of 3C 58 between 327 MHz and 4.9 GHz, $\alpha_{0.33}^{4.9}$, shown in gray scale. The FWHM resolution is $8\rlap{.}{''}3$ (shown at lower left). For reference, the 4%, 8%, and 16% contours from the total intensity image at 327 MHz are shown also.

tude calibration. This value is consistent with $\alpha_{0.04}^{15} = -0.10 \pm 0.02$, given by Green (1986).

We also reedited and reimaged the data of Reynolds & Aller (1988) and made a spectral-index image between 327 MHz and 4.9 GHz, $\alpha_{0.33}^{4.9}$, which is shown in Figure 5. Again, no particular features are visible in the body of the nebula, and no steepening toward the edge is observed. The mean and rms scatter of the spectral index over the central region of 3C 58 are -0.051 and 0.014, respectively. There is a very slight suggestion of a steepening of the spectral index near the filaments of less than 0.02, which is likely not real, since systematic sources of error, in particular image fidelity limits (see e.g., Perley 1999), introduce errors in the spectral index at this level that are likely correlated with the structure in the image itself. The integrated value of $\alpha_{0.33}^{4.9}$ is -0.06 ± 0.03, consistent with the above value from Green (1986).

4. EXPANSION OF 3C 58

In order to determine the rate of expansion of the synchrotron nebula, we compared our results with those from the aforementioned observations in 1984 by Reynolds & Aller (1988), and from observations in 1972 by Wilson & Weiler (1976). We reedited and reimaged both these sets of observations using maximum entropy method (MEM) deconvolution. In Table 1, we give details of the images used for determining the expansion. All the images at 1.4 and 5 GHz have been corrected for the attenuation of the

respective primary beam patterns (at lower frequencies, the correction is negligible). Our goal is to determine the expansion speed of the radio nebula. Since there are few well-defined compact features, we choose to measure the expansion not by determining the proper motion of individual features, but by determining an overall statistical scaling between our images. We accomplish this by using the MIRIAD task IMDIFF, which calculates how to make one image most closely resemble another by calculating unbiased estimators for the scaling in size, e, the scaling and the offset in flux density, A and b, respectively, and the offsets in R.A. and decl., x and y, respectively, needed to make the second image most closely resemble the first. We are chiefly interested in the expansion factor e, but because of uncertainties in flux calibration, absolute position, and image zero-point offsets caused by missing short spacings, we determine all parameters. This method was developed by Tan & Gull (1985), and more details of its use in a similar situation are given by Bietenholz et al. (1991).

Since we have shown above that the radio spectral index is uniform to within the uncertainties, images at any two frequencies v_1 and v_2 should closely resemble one another, except for a flux-scaling factor, which is given by $(v_1/v_2)^\alpha$, where α is the spectral index. Thus, we can usefully compare images taken at different observing frequencies to test for expansion.

We ran IMDIFF on various combinations of the above images, always with both images convolved to the same effective resolution, to get the expansion factors shown in Table 2. In order to estimate the uncertainty in our calculation of e, we also ran IMDIFF on two pairs of (almost) contemporaneous images, for which e should be 0.0. They are the expansion between 1.4 and 4.9 GHz at essentially the same epoch, and the expansion between a CLEAN and a MEM image of the 1973 4.9 GHz data, and the results are shown in the last two lines in Table 2. In both of these test cases, we obtain expansions of less than 0.2%, which suggests that the uncertainties in our expansion factors are of this order.

In order to determine the expansion speed, we fit a straight line through the first seven expansion factors in Table 2 by weighted least squares. The expansion for zero time difference must be 0.0, so we constrain the fit line to pass through the origin. Since we do not have formal uncertainties in the expansion factor, we use the weights listed in Table 2, which we derived as follows: it seems reasonable to suppose that the uncertainty in the expansion factor is proportional to the rms of the residuals of the IMDIFF fit, σ_{fit}, divided by the average brightness in the images—more flux

TABLE 1

IMAGES USED FOR THE EXPANSION DETERMINATION

Date	Telescope	Frequency (MHz)	$S_{\text{total}}^{\text{a}}$ (Jy)	Image rms (mJy per beam)	Convolving Beam (arcsec $\times$ arcsec, at deg)	Reference
1973 Feb–Jun	WSRT	4995	30.1	2.44	8.3 × 8.3	1
1973 Dec 15	WSRT	1415	33.1	1.35	22.7 × 20.9, at 0.0	1
1984 Jan–Aug	VLA	4866	29.5	0.43	8.3 × 8.3	2
	VLA	4866	29.5	1.71	17.7 × 17.4, at −7.5	2
1984 Jan–Dec	VLA	1446	33.9	0.49	17.7 × 17.4, at −7.5	2
1998 Oct 1	VLA	327	33.0	1.17	17.7 × 17.4, at −7.5	3
1998 Mar–Oct......	VLA	327	34.0	0.58	8.3 × 8.3	4

$^{\text{a}}$ S_{total} is the total cleaned flux density in the image.
REFERENCES.—(1) Wilson & Weiler 1976; (2) Reynolds & Aller 1988; (3) This paper, B-array only; (4) This paper, A and B arrays

TABLE 2

EXPANSION OF 3C 58

FIRST IMAGE		SECOND IMAGE		Resolution[b] (arcsec)	Time Interval (yr)	Change in Size (%)	rms of Fit (mJy beam^{-1})	Weight[c]
Year[a]	Frequency (MHz)	Year[a]	Frequency (MHz)					
1984.39	1.4	1998.75	0.3	17	14.4	0.80	1.4	1.1
1984.27	4.9	1998.46	0.3	8	14.2	0.45	0.6	1.7
1973.96	1.4	1998.75	0.3	21	24.8	0.80	3.0	0.5
1973.96	1.4	1984.39	1.4	21	10.4	−0.10	2.2	0.9
1973.96[d]	1.4	1984.39[d]	1.4	21	10.4	0.05	1.8	1.3
1973.29[d]	4.9	1998.46[d]	0.3	8	25.2	0.15	0.9	0.8
1973.29[d]	4.9	1984.27[d]	4.9	8	11.0	−0.10	0.7	1.3
The results below are included as a check								
1984.27	4.9	1984.39	1.4	17	0.1	−0.20	1.4	1.4
1973.27[e]	4.9	1973.27[e]	4.9	8	0.0	0.20	0.9	0.8

[a] For observations involving multiple arrays, the date given is the average over all the arrays, weighted by the length of the individual array observing runs.
[b] The rounded average resolution, see Table 1.
[c] These are the weights used for fitting the overall expansion; see text for details.
[d] These images have been high-pass filtered using a circular Gaussian of FWHM 60″.
[e] This line pertains to the difference between CLEAN and MEM images from the same data

in the image allows a relatively better fit for the same rms. Since the total flux density is roughly the same in all the images, the average brightness is inversely proportional to the number of beam areas over the source. It also seems reasonable that the uncertainty is inversely proportional to the square root of the number of beam areas in the fitting region, $A_{\text{fitting region}}$. We thus adopt as the weight

$$W = \frac{1}{\sigma_{\text{fit}}^2 A_{\text{fitting region}}}. \qquad (1)$$

For the 5 GHz, 1973 Westerbork Synthesis Radio Telescope (WSRT) data, we use only expansions derived from a version of the image high-pass filtered with a Gaussian of 1′ FWHM, since this image has evident short-spacing problems (Wilson & Weiler 1976). The points, as well as the weighted least-squares fit, are plotted in Figure 6.

The straight-line fit to the data in Table 2 by weighted least squares is plotted as the solid line in Figure 6. The slope, or average expansion speed, that we obtain from the fit is $(0.020 \pm 0.008)\%$ yr^{-1}, which corresponds to $\sim 910 \pm 360$ and 550 ± 220 km s^{-1} along the major and minor axes of the nebula, respectively. We can estimate the uncertainties from the scatter of the data points about the fit line, and we find that a $W = 1$ corresponds to an uncertainty of 0.34% in the expansion factor. Our two check points, which measure the expansion between almost simultaneous images (the last two lines of Table 2), are indeed consistent with an expansion of 0.0, as they should be. We also note that an unweighted fit gives almost the same expansion speed and uncertainty.

Our measured expansion speed (solid line in Fig. 6) is much less than would be expected for an undecelerated expansion of 3C 58 since 1181 A.D. The undecelerated "historical" expansion speed would be 0.124% yr^{-1} and is plotted as the dashed line in Figure 6. In addition, in Figure 7, we show profiles drawn through the long axis of 3C 58 at 1.4 GHz in 1984 and at 0.3 GHz in 1998, and for comparison, a hypothetical profile that is generated by undecelerated expansion of the 1984 profile to 1998. This last can

be seen to be notably larger than the true 1998 profile, also indicating a lower than "historical" expansion speed.

The nebular structure is dominated by the relatively sharp outer edges rather than by any well-defined filaments or clumps, so our expansion results derive in considerable part from the overall extent of the nebula. Unfortunately, this makes our expansion results sensitive to short-spacing problems and also to the accuracy of the beam corrections, especially at 5 GHz, where the VLA and WSRT primary beams are 825″ and 650″ FWHM, respectively. Because of this, we cannot exclude the presence of systematic biases in our results. However, we feel that the aggregate expansion speed, which is derived from a variety of combinations of
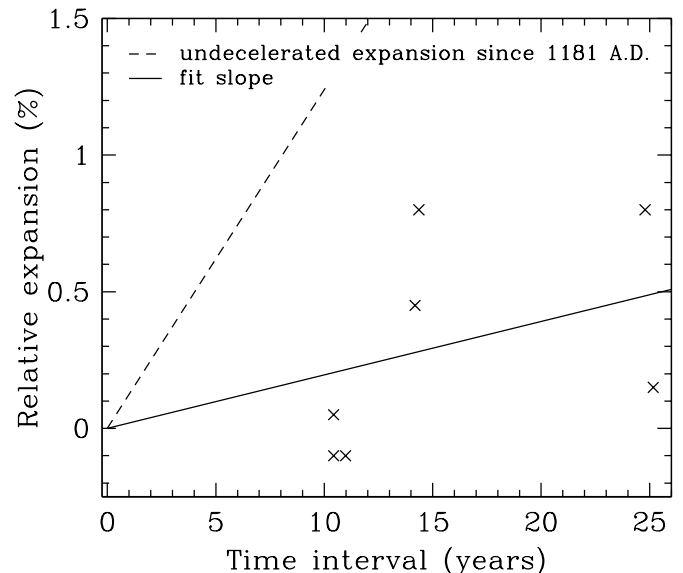

FIG. 6.—Expansion of 3C 58 over various time intervals. The points plotted represent the expansion required by IMDIFF over the pairs of observations from Table 2, excluding the last two check points. The solid line indicates the fit expansion speed of $(0.020 \pm 0.008)\%$ yr^{-1}, and the dashed line indicates the expansion of 0.124% yr^{-1} expected for undecelerated expansion since 1181 A.D.
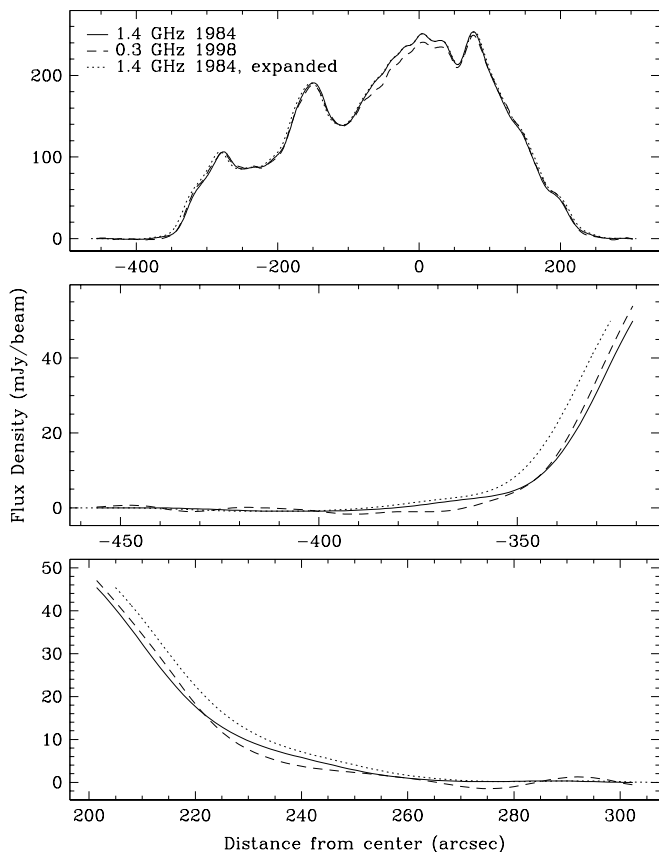
FIG. 7.—Profiles through 3C 58. The top panel shows the profile through 3C 58, drawn at P.A. −86°, i.e., through the long axis of the nebula. The solid line represents the flux density at 1.4 GHz in 1984. The dashed line represents the flux density at 0.3 GHz in 1998, multiplied by a flux density scaling factor so as to most closely match the 1984 profile (the scaling factor was determined by IMDIFF, see text § 4). The dotted line, drawn for comparison, represents the 1984 data homologously expanded by 1.74%, which is the expected amount if 3C 58 is the undecelerated remnant of SN 1181. The middle and the bottom panel are magnified regions of the profile in the top panel, showing details of the eastern and western limbs of 3C 58, respectively. The FWHM resolution is 17″.7 × 17″.4, at −7°.5.

different epochs, resolutions, telescopes, and frequencies, is unlikely to be greatly biased.

5. DISCUSSION

We measure an expansion rate of the radio nebula for 3C 58 of $(0.020 \pm 0.008)\%$ yr^{-1} (corresponding to $\sim 910 \pm 360$ and 550 ± 220 km s^{-1} along the major and minor axes of the nebula, respectively). This is much smaller than would be expected if 3C 58 were indeed the undecelerated remnant of SN 1181, which would require an expansion of 0.124% yr^{-1} (~ 5500 and ~ 3300 km s^{-1} along the major and minor axes, respectively). Conversely, our measured expansion rate suggests an age for 3C 58 of 5000 yr with a 3 σ lower limit of 2250 yr, which is incompatible with the generally accepted association with SN 1181. Although we cannot entirely rule out systematic sources of error in our determination of the expansion, we think it unlikely that they are large enough to make our results compatible with an expansion age of ~ 820 yr.

This low expansion speed is corroborated by the proper motions of optical filaments: Fesen, Kirshner, & Becker (1988) and van den Bergh (1990) looked for such proper motions and failed to find any larger than 0″.07 yr^{-1}. Fesen

(1983) measured optical radial velocities for several filaments in 3C 58. The largest radial velocities he measured were ~ 900 km s^{-1} for filaments situated near the projected center of the nebula, where the expansion is along the line of sight, and thus where the expansion speed is expected to be approximately equal to the radial velocity. This is also substantially lower than the $\gtrsim 3000$ km s^{-1} implied by undecelerated expansion and a distance of 3.2 kpc. (We note that Fesen, who used a somewhat smaller distance to 3C 58 of 2.6 kpc, reconciled these radial velocities with an age of 820 yr by suggesting that substantial deceleration had taken place, and that the average speed since 1181 A.D. was ~ 3000 km s^{-1}.) In order to determine an expansion age from this radial velocity, we need to know the radius at which the measured filament lies from the center of the nebula. If we take this radius to be the mean projected radius of ~ 4 pc, these radial velocities also imply a large age of ~ 4400 yr, but since the optical emission is faint, those radial velocities may have been measured for filaments nearer the center of the nebula, and thus a smaller radius and consequently a smaller age is possible. However, we consider it unlikely that the largest radial velocities were measured for filaments only ~ 1 pc from the center of the nebula. If 3C 58 is associated with SN 1181, all this evidence suggests that it must have been greatly decelerated.

The simplest solution to these inconsistencies is to suggest that 3C 58 is not the remnant of SN 1181. This also alleviates the difficulties in accounting for the very sharp and rather low frequency spectral break observed in 3C 58 (Woltjer et al. 1997; Green & Scheuer 1992). Note that a lower value for the somewhat uncertain distance estimate for 3C 58 would reduce the age determined from the radial velocities, but not that determined from the proper motions, so that is not a solution. The positional coincidence between SN 1181 and 3C 58, however, was confirmed by a recent reexamination (Stephenson & Green 1999), and so if 3C 58 is not to be associated with SN 1181, one must ask where the remnant of SN 1181 is, since there are no other obvious candidates, and since it seems unlikely that the remnant would already be too faint to observe at an age of only 820 yr.

Van den Bergh (1990) suggests that the presently visible optical filaments predate the supernova event, and are quasi-stationary but energized by the passing supernova shock wave. It is not clear that the low expansion rate of the synchrotron bubble can be accounted for in this way, since it seems unlikely that these preexisting filaments, which have a low filling factor, would be able to confine the synchrotron bubble. While some coupling between the synchrotron bubble and the thermal filaments would be expected, since the magnetic field in the bubble would wrap around the thermal filaments, one would expect the synchrotron bubble to rapidly expand beyond the filaments, along with the rest of the supernova ejecta. The outside edge of the visible synchrotron bubble should be expanding at least at the speed of the local ejecta, which would be ~ 4000 km s^{-1} for undecelerated expansion. Should preexisting filaments nonetheless be somehow confining the synchrotron bubble, then the filaments should be accelerated. The current measurements, unfortunately, do not have the precision necessary to determine if this is the case.

A possible explanation for slow-moving filaments is the following: the magnetic field wraps around the preexisting filaments and causes an intensification of the synchrotron

emissivity in their vicinity, which is why these filaments are visible in radio synchrotron emission. If the structure of the radio nebula is dominated by these irregularities, then our determination of the expansion would determine the expansion precisely of the filaments and *not* of the synchrotron bubble as a whole. We note that expansion speeds that we measure at lower effective resolutions tend to be slightly smaller than those at larger resolutions, as would be expected in this case, but even the measured expansions at lower resolutions are far below the expected values for undecelerated expansion. Furthermore, profiles through the images do not support the conjecture of quasi-stationary filaments in an expanding bubble: the profiles displayed in Figure 7 show that even the expansion of the edge of the nebula appears to be considerably less than is expected from undecelerated expansion.

Let us turn to some general physical considerations about the synchrotron bubble. The pressure in the synchrotron bubble is relatively high: standard arguments give a minimum pressure of greater than 10^{-10} dyn cm^{-2}. This is the minimum pressure of the synchrotron fluid assuming a filling factor of 1.0 and a line-of-sight depth equal to the long axis of the projected nebula. Both a lower filling factor and the admixture of any thermal material would raise the pressure, and we think it unlikely that the line-of-sight dimension is much larger than the long axis of the projected nebula.

The slow expansion of the bubble therefore necessitates some confining pressure, since the sound and Alfvén velocities in the bubble are also high. This leads to the question of what surrounds the presently visible nebula. The three possibilities are (1) the ISM, (2) the wind bubble of the presupernova progenitor of SN 1181, or (3) a freely expanding stellar envelope thrown off in the supernova explosion. This last might be expected, since the total energy in the visible remnant is far below the expected energy of 10^{51} ergs released in a supernova for any reasonable mass in the filaments. This last situation does seem to obtain in the Crab Nebula, where strong circumstantial evidence points to the existence of such a freely expanding stellar envelope (Hester et al. 1996; Sankrit & Hester 1997), even though the radio emission from this shell has so far eluded detection (Bietenholz et al. 1997; Frail et al. 1995), and the direct optical detection is controversial.

The static pressure of any of these three exterior media, p_{ext}, is expected to be considerably smaller than the minimum pressure in the synchrotron bubble;

$$p_{ext} = 1.4 \times 10^{-12} \text{ dyn cm}^{-2}(n/1 \text{ cm}^{-3})(T/10^4 \text{ K}) , \quad (2)$$

where n is the number density and T is the temperature. This suggests that the synchrotron bubble is confined by ram pressure as it expands into the surrounding material. We are then brought to a crucial difference between 3C 58 and the Crab Nebula: in the case of the Crab, the synchrotron bubble has been accelerated since the supernova event (Bietenholz et al. 1991), and is therefore expanding *into* the stellar envelope, and confined by the ram pressure of this expansion. In the case of 3C 58, by contrast, the synchrotron bubble is expanding considerably more *slowly* than any freely expanding material thrown off in SN 1181, and cannot therefore be confined by ram pressure in any freely expanding ejecta.

This implies for 3C 58 that there is no freely expanding envelope, making it a very low-energy supernova event, or

that the envelope has been greatly decelerated, which seems unlikely in light of the nondetection of any shell emission exterior to the synchrotron remnant, or that it is not the remnant of SN 1181. The ram pressure required suggests that the external medium have a number density, n_{ext}, of

$$n_{ext} \sim 0.1 \text{ cm}^{-3} (v_{shock}/1000 \text{ km s}^{-1})^2 (m/m_H) , \quad (3)$$

where v_{shock} is the difference in velocity between the synchrotron bubble and the undisturbed exterior medium, and m is the mean mass per particle.

A possible scenario would be that 3C 58 is the composite remnant of a binary where both stars have undergone supernova explosions, with the earlier supernova leaving the slowly expanding remnant, and the later, low-energy one providing the historical supernova event in 1181 A.D. This scenario seems rather contrived, since having two supernovae within a few thousand years of one another is quite unlikely.

We turn to the nondetection of any shell emission. If there were an envelope ejected in SN 1181, as discussed above, it would have been decelerated by at least a factor of 3, which in turn suggests that it would have already swept up considerable external material, and be well into the Sedov phase of its evolution. It is then surprising that the radio brightness of this exterior shell is considerably less than that of the faintest known shells. Again, it is instructive to point out the difference between 3C 58 and the Crab Nebula. Also, for the Crab, radio emission from the shell has not yet been detected to similar limits in surface brightness, but the envelope is still in the free-expansion phase and is not expected to have converted much of its energy into relativistic particles, and therefore is expected to be fainter than most shell remnants.

Could a shell for 3C 58 be masked because it is largely coincident with the synchrotron nebula? Shock-accelerated radio-synchrotron emitting electrons typically produce radio emission with a spectral index $\alpha \sim -0.6$. Our spectral index results, however, indicate that there is no significant radio emission with $\alpha = -0.6$ near the edge of the nebula, since we observe no steepening of the spectrum there. Also, the total flux density that we measure at 74 MHz gives an integrated spectral index no steeper than that at higher frequencies, contrary to what would be expected if there were a steep spectrum component present.

Both $\alpha_{0.07}^{0.33}$ and $\alpha_{0.33}^{4.9}$ show no spatial variation over the nebula, $\alpha_{0.33}^{4.9}$ showing rms variations of only less than 0.05. The uniformity of the spectral index suggests that a single acceleration mechanism is responsible for all the radio-emitting electrons. This is thought to be an as yet undetected pulsar, although there are a number of problems with 3C 58 in this regard. Recent X-ray results by Bocchino et al. (2001) do not show the expected blackbody X-ray emission from the neutron star. No pulsed emission has so far been found at any wavelength, although in a deep-radio image, Frail & Moffett (1993) detected a "wisplike" feature, similar to ones usually associated with the termination shock of a pulsar wind.

6. A SHELL AROUND 3C 58

In the case of the Crab Nebula, there is substantially less kinetic energy in the remnant than the 10^{51} ergs expected from a Type II supernova. This has suggested the existence of a rapidly moving shell around the currently visible remnant that carries the excess energy and also confines the

relatively high-pressure synchrotron bubble. Much observational effort has been expended in search of this shell around the Crab, but no shell has yet been detected in the radio, ruling out any radio emission with a surface brightness much less than that of the faintest known young shell remnant, SN 1006 (Frail et al. 1995; Bietenholz et al. 1997). However, in the case of the Crab, circumstantial evidence for the existence of expanding material outside the currently visible nebula has been made from *Hubble Space Telescope* observations (Hester et al. 1996), which show the Rayleigh-Taylor unstable interface between the high-pressure synchrotron bubble and the hydrogen shell.

In the case of 3C 58, there is a similar deficit in energy, especially in view of the low expansion velocity of both the synchrotron bubble and the optical filaments, and so a rapidly moving shell might also be expected exterior to the currently visible nebula. Several searches for a radio shell around 3C 58 have been made, notably by Reynolds & Aller (1985), and no sign of radio emission from a shell has yet been detected.

Our 327 MHz results give a sensitive upper limit to the radio emission from a putative shell of 1×10^{-21} W m^{-2} Hz^{-1} sr^{-1} at that frequency. Scaling with an assumed shell spectral index of -0.6, this is equivalent to 4×10^{-22} W m^{-2} Hz^{-1} sr^{-1} at 1.4 GHz, thus very slightly more sensitive than the earlier limit of 4.7×10^{-22} W m^{-2} Hz^{-1} sr^{-1} obtained by Reynolds & Aller (1985). We are, however, more sensitive to steep-spectrum shells and also to larger shells because of our larger field of view at 327 MHz. We note that, even on our 74 MHz images, where the primary beam radius is $\sim 5°$, there is no sign of shell emission, albeit at a lower sensitivity than at 327 MHz. A sensitivity to larger shells may be germane if 3C 58 is, in fact, older than SN 1181, since at 10,000 km s^{-1}, a 3500 yr old shell at 3.2 kpc would have an angular diameter of 1°.2.

7. CONCLUSIONS

New observations at 74 and 327 MHz and reanalysis of older observations dating back to 1974 indicate that:

1. 3C 58 has a flat spectral index of $\alpha_{0.07}^{0.33} = -0.05$, with little variation over the nebula.
2. The expansion of the synchrotron nebula is much slower than expected for an explosion date in 1181 A.D., with constant undecelerated expansion since then. A possible explanation is that 3C 58 is not the remnant of SN 1181 but is far older, with an age of ~ 5000 yr; however, we are reluctant to abandon the generally accepted association until a better understanding of the dynamics of plerions is available, and a better candidate remnant for SN 1181 is found. An alternate explanation is that 3C 58 has been greatly decelerated.
3. As in the Crab Nebula, any nonthermal emission from a shock wave outside the observable plerion has a very low surface brightness of less than 1×10^{-22} W m^{-2} Hz^{-1} sr^{-1}. If 3C 58 has been greatly decelerated as suggested in item 2 above, then one would expect radio emission from such a shock wave.

We close by summarizing several apparent inconsistencies in the observational material on 3C 58. First, the measured low proper motions, both in the radio and in the optical, along with the low synchrotron break frequency, suggest an age much older than 820 yr. On the other hand, the positional association with SN 1181 seems secure, and no other remnant has been identified for this historical supernova. The radio spectral index is very uniform, suggesting a common source for the radio-emitting electrons, namely a pulsar wind, yet the postulated pulsar has escaped detection and the expected X-ray emission from the hot surface of the neutron star has not been detected. Finally, the currently observable remnant contains only a small fraction of the kinetic energy expected from a Type II supernova. Unless SN 1181 was an anomalously low energy event, a shell consisting of the rapidly moving external layers of the star would be expected to carry the balance of the kinetic energy. Such a shell has not been detected, and would be anomalously faint in comparison to other known shells. We hope that future study will allow us a more complete and consistent picture of this fascinating object.

REFERENCES

Aller H. D., Aller, M. F., & Reynolds, S. P. 1986, BAAS, 18, 1052
Aller, H. D., & Reynolds, S. P. 1985, in The Crab Nebula and Related Supernova Remnants, ed. M. C. Kafatos & R. B. C. Henry (Cambridge: Cambridge Univ. Press), 75
Baars, J. W. M., Genzel, R., Pauliny-Toth, I. I. K., & Witzel, A. 1977, A&A, 61, 99
Bietenholz, M. F., Kassim, N., Frail, D. A., Perley, R. A., Erickson, W. C., & Hajian, A. R. 1997, ApJ, 490, 291
Bietenholz, M. F., Kronberg, P. P., Hogg, D. E., & Wilson, A. S. 1991, ApJ, 373, L59
Bocchino, F., Warwick, R. S., Marty, P., Lumb, D., Becker, W., & Pigot, C. 2001, A&A, 369, 1078
Clark, D. H., & Stephenson, F. R. 1977, The Historical Supernovae (Oxford: Pergamon)
Fesen, R. A. 1983, ApJ, 270, L53
Fesen, R. A., Kirshner, R. P., & Becker, R. H. 1988, in IAU Colloq. 101, Supernova Remnants and the Interstellar Medium, ed. R. S. Roger & T. L. Landecker (Cambridge: Cambridge Univ. Press), 55
Frail, D. A., Kassim, N. E., Cornwell, T. J., & Goss, W. M. 1995, ApJ, 454, L129
Frail, D. A., & Moffett, D. A. 1993, ApJ, 408, 637
Green, D. A. 1986, MNRAS, 218, 533

Green, D. A. 1987, MNRAS, 225, 11
Green, D. A., & Scheuer, P. A. G. 1992, MNRAS, 258, 833
Hester, J. J., et al. 1996, ApJ, 456, 225
Perley, R. A. 1999, in ASP Conf. Ser. 180, Synthesis Imaging in Radio Astronomy II, , ed. G. B. Taylor, C. L. Carilli, & R. A. Perley (San Francisco: ASP), 383
Reynolds, S. P., & Aller, H. D. 1985, AJ, 90, 2312
———. 1988, ApJ, 327, 845
Roberts, D. A., Goss, W. M., Kalberla, P. M. W., Herbstmeier, U., & Schwarz, U. J. 1993, A&A, 274, 427
Salvati, M., Bandiera, F., Pacini, F., & Woltjer, L. 1998, J. Italiana Astron. Soc., 69, 1023
Sankrit, R., & Hester, J. J. 1997, ApJ, 491, 796
Stephenson, F. R., & Green, D. A. 1999, Astron. & Geophys., 40, 27
Tan, S. M., & Gull, S. F. 1985, MNRAS, 216, 949
van den Bergh, S. 1990, ApJ, 357, 138
Weiler, K. W., & Panagia, N. 1978, A&A, 70, 419
Weiler, K. W., & Seielstad, G. A. 1971, ApJ, 163, 455
Weiler, K. W., & Sramek, R. A. 1988, ARA&A, 26, 295
Wilson, A. S., & Weiler, K. W. 1976, A&A, 49, 357
Woltjer, L., Salvati, M., Pacini, F., & Bandiera, R. 1997, A&A, 325, 295